

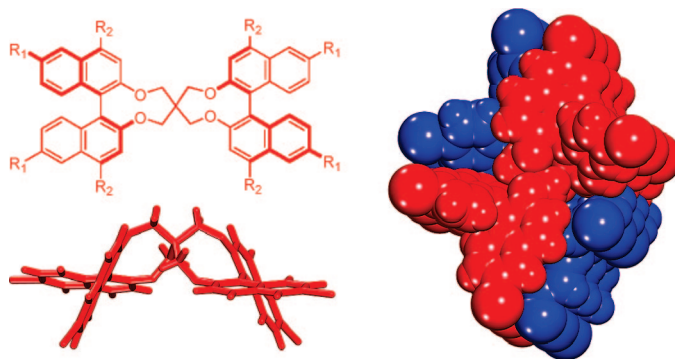
Synthesis and Structure of Spirocyclic Tetraethers Derived from [1,1'-Binaphthalene]-2,2'-diol and Pentaerythritol

Tao Tu, Thierry Maris, and James D. Wuest*

Département de Chimie, Université de Montréal, Montréal, Québec H3C 3J7, Canada

james.d.wuest@umontreal.ca

Received January 28, 2008



Molecular scaffolds that have well-defined geometries, are easy to synthesize and functionalize, and can hold attached sites of molecular recognition in suitable orientations are useful tools in various areas of science and technology. The utility of the tetraphenyl ether of pentaerythritol (**4**) as a scaffold in crystal engineering led us to study rigidified analogue SBINOX (**5**), the spirocyclic tetraether derived from pentaerythritol and [1,1'-binaphthalene]-2,2'-diol (BINOL). We have found that SBINOX (**5**) and derivatives can be prepared conveniently in acceptable yields and in stereoisomerically pure (*S,S*), (*R,S*), and (*R,R*) forms. X-ray crystallographic studies have revealed that the benzannulated 9-membered dioxonane rings in these structures adopt characteristic conformations of C_1 symmetry. Intraannular C–H \cdots O interactions help maintain the conformations of the individual rings, and the geometry of the spirocyclic SBINOX core is also controlled in part by distinctive short interannular C–H \cdots O and C–H \cdots π interactions. Despite the inherent flexibility of the dioxonane rings, derivatives of SBINOX (**5**) can be expected to orient peripheral substituents in preferred ways, making SBINOX a potentially useful scaffold for applications in drug discovery, crystal engineering, and other fields.

Introduction

Libraries of compounds that can be created by attaching diverse functional groups to particular molecular scaffolds are useful tools in many areas of science and technology. In drug discovery, for example, bioactive molecules can be mimicked by using derivatized scaffolds that display carefully selected functional groups in orientations favoring interaction with specific receptors or enzymes.¹ In addition, recent advances in engineering molecular crystals and building other ordered materials have exploited a related strategy for ensuring that neighboring molecules associate according to plan. The fundamental units of construction in this strategy, which have been called tectons,² can be created from suitable molecular scaffolds by attaching functional groups that engage in strong directional

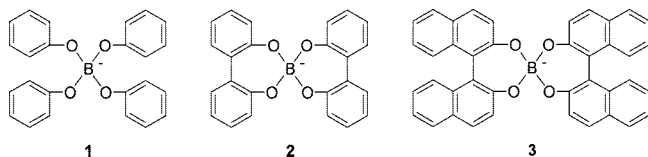
intermolecular interactions, thereby ensuring that neighboring tectons are held in predetermined positions.^{3,4} Privileged scaffolds for use in drug discovery, crystal engineering, and related applications should have well-defined geometries, be easy to synthesize and functionalize, and hold the attached sites of molecular recognition in suitable orientations.

(1) For representative recent references, see: Comer, E.; Rohan, E.; Deng, L.; Porco, J. A., Jr. *J. Org. Lett.* **2007**, *9*, 2123–2126. Meutermans, W.; Le, G. T.; Becker, B. *ChemMedChem* **2006**, *1*, 1164–1194. Ganesan, A. In *Exploiting Chemical Diversity for Drug Discovery*; Entzeroth, M., Bartlett, P. A., Eds.; Royal Society of Chemistry: Cambridge, U.K., 2006; pp 91–111. Timmer, M. S. M.; Verhelst, S. H. L.; Grotenbreg, G. M.; Overhand, M.; Overkleef, H. S. *Pure Appl. Chem.* **2005**, *77*, 1173–1181. Dallinger, D.; Kappe, C. O. *Pure Appl. Chem.* **2005**, *77*, 155–161.

(2) Simard, M.; Su, D.; Wuest, J. D. *J. Am. Chem. Soc.* **1991**, *113*, 4696–4697.

(3) For recent reviews, see: Wuest, J. D. *Chem. Commun.* **2005**, 5830–5837. Hosseini, M. W. *Acc. Chem. Res.* **2005**, *38*, 313–323.

An instructive series of increasingly sophisticated scaffolds for use in crystal engineering, materials science, and other areas is provided by borates **1**–**3**.^{5,6} All are readily synthesized from boric acid and the corresponding phenols, but compounds **2** and **3** are particularly attractive because they offer higher rigidity and therefore allow substituents located on the peripheral aryl groups to be positioned more reliably. Moreover, spiroborate **3** is chiral and provides a configurationally stable scaffold available as a racemate or as pure (*S,S*) and (*R,R*) enantiomers.⁶ The alternative meso (*R,S*)-isomer has not been observed.⁶



These features encouraged us to use an analogous approach to introduce rigidity and chirality into the tetraphenyl ether of pentaerythritol (**4**), a scaffold previously used to engineer molecular crystals held together by hydrogen bonds and other interactions.^{7–12} In this paper, we report the synthesis and structure of spirocycle **5** (SBINOX),¹³ a tetraether derived from pentaerythritol and [1,1'-binaphthalene]-2,2'-diol (BINOL). In addition, we describe tetrabromide **6** and octabromide **7**, which are attractive precursors for the synthesis of various functionalized derivatives of SBINOX (**5**). Together, this work provides a foundation for future studies of tectons derived from SBINOX (**5**) by the attachment of functional groups that engage in strong directional intermolecular interactions.

(4) For other recent references, see: Maly, K. E.; Gagnon, E.; Maris, T.; Wuest, J. D. *J. Am. Chem. Soc.* **2007**, *129*, 4306–4322. Roques, N.; Maspocho, D.; Wurst, K.; Ruiz-Molina, D.; Rovira, C.; Veciana, J. *Chem. Eur. J.* **2006**, *12*, 9238–9253. Lebel, O.; Maris, T.; Perron, M.-È.; Demers, E.; Wuest, J. D. *J. Am. Chem. Soc.* **2006**, *128*, 10372–10373. Sokolov, A. N.; Friščić, T.; MacGillivray, L. R. *J. Am. Chem. Soc.* **2006**, *128*, 2806–2807. Pigge, F. C.; Dighe, M. K.; Rath, N. P. *Cryst. Growth Des.* **2006**, *6*, 2732–2738. Saha, B. K.; Nangia, A.; Nicoud, J.-F. *Cryst. Growth Des.* **2006**, *6*, 1278–1281. Jayaraman, A.; Balasubramanian, V.; Valiyaveetil, S. *Cryst. Growth Des.* **2006**, *6*, 636–642. Suslick, K. S.; Bhyrappa, P.; Chou, J.-H.; Kosal, M. E.; Nakagaki, S.; Smithenry, D. W.; Wilson, S. R. *Acc. Chem. Res.* **2005**, *38*, 283–291. Aakeröy, C. B.; Desper, J.; Urbina, J. F. *Chem. Commun.* **2005**, 2820–2822. Braga, D.; Brammer, L.; Champness, N. R. *CrystEngComm* **2005**, *7*, 1–19. Sisson, A. L.; del Amo Sanchez, V.; Magro, G.; Griffin, A. M. E.; Shah, S.; Charmant, J. P. H.; Davis, A. P. *Angew. Chem., Int. Ed.* **2005**, *44*, 6878–6881. Malek, N.; Maris, T.; Perron, M.-È.; Wuest, J. D. *Angew. Chem., Int. Ed.* **2005**, *44*, 4021–4025. Voogt, J. N.; Blanch, H. W. *Cryst. Growth Des.* **2005**, *5*, 1135–1144. Lee, S.-O.; Shacklady, D. M.; Horner, M. J.; Ferlay, S.; Hosseini, M. W.; Ward, M. D. *Cryst. Growth Des.* **2005**, *5*, 995–1003. Custelcean, R.; Gorbunova, M. G.; Bonnesen, P. V. *Chem. Eur. J.* **2005**, *11*, 1459–1466. Moorthy, J. N.; Natarajan, R.; Venugopalan, P. *J. Org. Chem.* **2005**, *70*, 8568–8571. Saied, O.; Maris, T.; Wang, X.; Simard, M.; Wuest, J. D. *J. Am. Chem. Soc.* **2005**, *127*, 10008–10009. Malek, N.; Maris, T.; Simard, M.; Wuest, J. D. *J. Am. Chem. Soc.* **2005**, *127*, 5910–5916. Soldatov, D. V.; Moudrakovski, I. L.; Ripmeester, J. A. *Angew. Chem., Int. Ed.* **2004**, *43*, 6308–6311. Alshahateet, S. F.; Nakano, K.; Bishop, R.; Craig, D. C.; Harris, K. D. M.; Scudder, M. L. *CrystEngComm* **2004**, *6*, 5–10.

(5) Voisin, E.; Maris, T.; Wuest, J. D. *Cryst. Growth Des.* **2008**, *8*, 308–318.

(6) Tu, T.; Maris, T.; Wuest, J. D. *Cryst. Growth Des.* **2008**, *8*, 1541–1546.

(7) Laliberté, D.; Maris, T.; Ryan, P. E.; Wuest, J. D. *Cryst. Growth Des.* **2006**, *6*, 1335–1340.

(8) Laliberté, D.; Maris, T.; Demers, E.; Helzy, F.; Arseneault, M.; Wuest, J. D. *Cryst. Growth Des.* **2005**, *5*, 1451–1456.

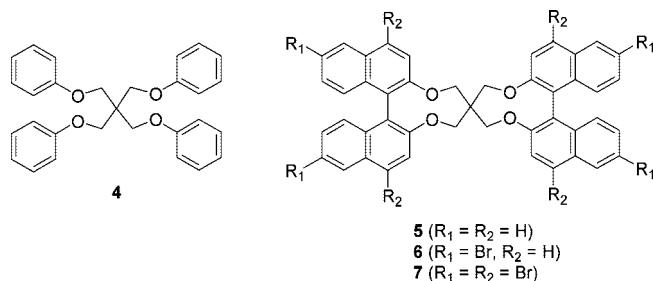
(9) Laliberté, D.; Raymond, N.; Maris, T.; Wuest, J. D. *Acta Crystallogr.* **2005**, *E61*, o601–o603.

(10) Laliberté, D.; Maris, T.; Wuest, J. D. *CrystEngComm* **2005**, *7*, 158–160.

(11) Laliberté, D.; Maris, T.; Wuest, J. D. *J. Org. Chem.* **2004**, *69*, 1776–1787.

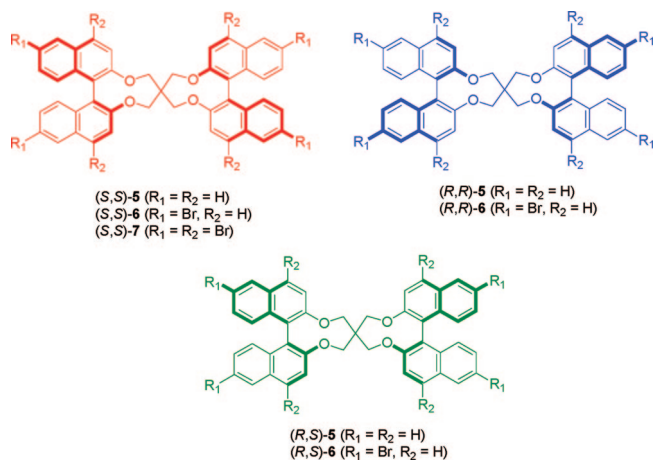
(12) Laliberté, D.; Maris, T.; Wuest, J. D. *Acta Crystallogr.* **2003**, *E59*, o799–o801.

(13) We use SBINOX to abbreviate the Chemical Abstracts name 5,5'-(6*H*,6'*H*)spirobi[4*H*-dinaphtho[2,1-*f*:1',2'-*h*][1,5]dioxin.



Results and Discussion

Synthesis of SBINOX (5) and Brominated Derivatives 6 and 7. A previous synthesis of SBINOX (**5**) was reported in 1971 by Smoliński and Deja,¹⁴ who obtained the compound in 8% yield by heating pentaerythrityl tetrabromide with the sodium salt of (\pm)-BINOL, followed by crystallization of the crude product. Analysis of stereomodels suggested to Smoliński and Deja that they had obtained a racemic mixture of the (*S,S*) and (*R,R*) enantiomers of SBINOX (**5**) rather than the meso (*R,S*) isomer, but the product was characterized only by IR spectroscopy, UV spectroscopy, and elemental analysis. To simplify subsequent structural drawings, (*S,S*) stereoisomers are drawn in red, (*R,R*) isomers in blue, and (*R,S*) isomers in green. The very low yield obtained by Smoliński and Deja may help account for the subsequent near absence of SBINOX (**5**) and its derivatives from the scientific literature,^{15,16} despite the intriguing potential of the scaffold.



To improve the yield, we took advantage of our earlier observation that tetraphenyl ethers of pentaerythritol can be made efficiently by heating the corresponding phenol, NaOH, and pentaerythrityl tetratosylate in DMF.¹¹ As expected, a similar reaction with (\pm)-BINOL provided crude SBINOX (**5**) in acceptable yield, and we found that even better results could be obtained by using K_2CO_3 in place of NaOH and by heating the mixture of reactants at 120 °C for 24 h. Under these conditions, (\pm)-BINOL was converted into crude SBINOX (**5**)

(14) Smoliński, S.; Deja, I. *Tetrahedron* **1971**, *27*, 1409–1413.

(15) Jamrozik, J. *J. Prakt. Chem.* **1985**, *327*, 1033–1036. Nowakowska, M.; Najbar, J.; Waligóra, B.; Smoliński, S. *Acta Phys. Polonica* **1974**, *A45*, 593–602.

(16) For a related spirocyclic ether derived from BINOL and pentaerythritol, see: Rajakumar, P.; Sekar, K.; Srinivasan, K. *Tetrahedron Lett.* **2005**, *46*, 1905–1907.

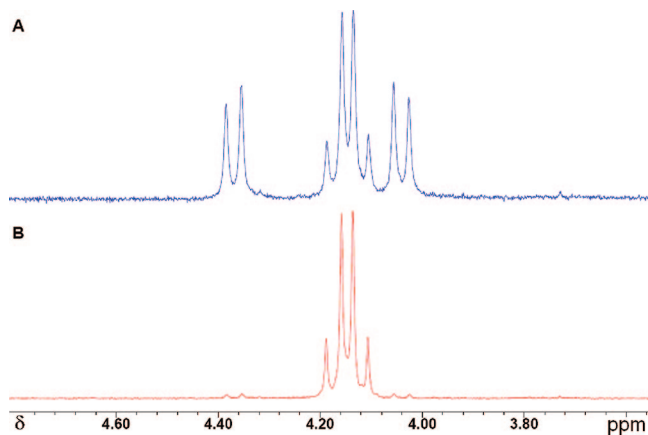


FIGURE 1. (A) View of part of the ^1H NMR spectrum (400 MHz, CDCl_3 , 298 K) of crude tetrabromide **6** derived from (\pm) -6,6'-dibromo[1,1'-binaphthalene]-2,2'-diol,¹⁷ showing a statistical ratio of the (S,S) , (R,S) , and (R,R) stereoisomers. (B) View of part of the ^1H NMR spectrum (400 MHz, CDCl_3 , 298 K) of (S,S) -tetrabromide **6** derived from $((S)$ -6,6'-dibromo[1,1'-binaphthalene]-2,2'-diol.¹⁷

in 85% yield, and (\pm) -6,6'-dibromo[1,1'-binaphthalene]-2,2'-diol¹⁷ provided crude tetrabromide **6** in 60% yield.

Examination of these crude materials by ^1H NMR spectroscopy at 298 K revealed that they were nearly statistical 1:2:1 mixtures of the (S,S) , (R,S) , and (R,R) stereoisomers. In the case of the crude tetrabromide **6** derived from (\pm) -6,6'-dibromo[1,1'-binaphthalene]-2,2'-diol,¹⁷ for example, the CH_2 group gave rise to two separate pairs of doublets of equal integration, one pair with doublets centered at δ 4.17 and 4.12 ($^2J = 11.9$ Hz), and the other with doublets centered at δ 4.38 and 4.04 ($^2J = 12.2$ Hz) (Figure 1A). The difference in the values of $\Delta\delta$ for each pair is relatively large (0.05 and 0.34), so the two stereoisomers must have conformations that orient the C–H bonds of the CH_2 groups in significantly different ways relative to the anisotropic effects of nearby naphthyl rings or to the lone pairs of adjacent atoms of oxygen.

The peaks were assigned by examining the products of the reactions of enantiomerically pure BINOL and its derivatives with pentaerythrityl tetrasylate under our standard conditions. For example, the reaction of (S) -6,6'-dibromo[1,1'-binaphthalene]-2,2'-diol¹⁷ yielded essentially pure (S,S) -tetrabromide **6** in 55% yield, and the ^1H NMR spectrum of the crude product showed almost exclusively the diagnostic pair of doublets at δ 4.17 and 4.12 (Figure 1B). The near-absence of the other pair demonstrated that (R,S) -tetrabromide **6** is not formed in significant amounts under these conditions and that racemization of either (S) -6,6'-dibromo[1,1'-binaphthalene]-2,2'-diol¹⁷ or tetrabromide **6** is negligible. Similar reactions with enantiomerically pure (S) -BINOL and (S) -4,4',6,6'-tetrabromo[1,1'-binaphthalene]-2,2'-diol^{18,19} provided the corresponding enantiomerically pure (S,S) -SBINOX $((S,S)$ -**5**), and (S,S) -octabromide **7** in 75% and 25% yields, respectively. Our method of synthesis thereby provides convenient access to SBINOX (**5**) and key derivatives in both racemic and enantiomerically pure forms.

(17) Deussen, H.-J.; Hendrickx, E.; Boutton, C.; Krog, D.; Clays, K.; Bechgaard, K.; Persoons, A.; Bjørnholm, T. *J. Am. Chem. Soc.* **1996**, *118*, 6841–6852. Sogah, G. D. Y.; Cram, D. J. *J. Am. Chem. Soc.* **1979**, *101*, 3035–3042.

(18) Hu, Q.-S.; Pugh, V.; Sabat, M.; Pu, L. *J. Org. Chem.* **1999**, *64*, 7528–7536.

(19) Cram, D. J.; Helgeson, R. C.; Peacock, S. C.; Kaplan, L. J.; Domeier, L. A.; Moreau, P.; Koga, K.; Mayer, J. M.; Chao, Y.; Siegel, M. G.; Hoffman, D. H.; Sogah, G. D. Y. *J. Org. Chem.* **1978**, *43*, 1930–1946.

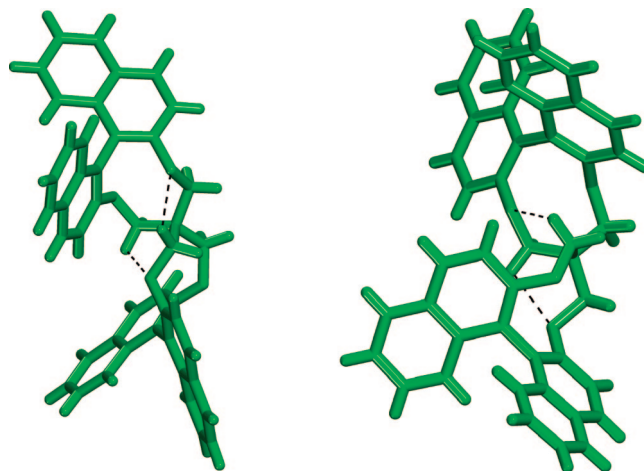


FIGURE 2. Two views of the molecular structure of meso (R,S) -SBINOX $((R,S)$ -**5**) as found in crystals grown from CH_2Cl_2 /hexane. For simplification, all atoms are drawn in green. The two shortest intramolecular C–H \cdots O interactions are highlighted by broken lines.

Direct bromination of SBINOX (**5**) was examined as an alternative route to derivatives **6** and **7**, but it yielded crude products that were hard to purify.

Structure of Meso (R,S) -SBINOX $((R,S)$ -5**).** Crude SBINOX (**5**), obtained as a statistical mixture of the (S,S) , (R,S) , and (R,R) isomers from the reaction of (\pm) -BINOL with pentaerythrityl tetrasylate, was crystallized by exposing a solution in CH_2Cl_2 to vapors of hexane. Contrary to the conclusions of Smoliński and Deja,¹⁴ the resulting crystals proved to consist solely of the meso (R,S) isomer, and the (S,S) and (R,R) isomers were absent. The crystals were found to belong to the orthorhombic space group $P2_12_12_1$.²⁰ Views of the structure appear in Figures 2–3, and crystallographic details are provided in Tables 1 and 2.

The central $\text{C}(\text{CH}_2\text{O})_4$ unit in meso (R,S) -SBINOX $((R,S)$ -**5**) has a slightly distorted tetrahedral geometry closely similar to that of acyclic analogues, such as the tetraphenyl ether of pentaerythritol (**4**) and its derivatives.^{9,12} In particular, the $\text{C}-\text{C}_{\text{core}}-\text{C}$ angles at the central carbon atom (C_{core}) of the pentaerythrityl core of meso (R,S) -SBINOX $((R,S)$ -**5**) range from $104.9(2)^\circ$ to $111.9(2)^\circ$, and the two independent $\text{C}-\text{C}_{\text{core}}-\text{C}$ angles in model **4** have similar values of $108.6(1)^\circ$ and $111.3(2)^\circ$. The principal difference between the cores of meso (R,S) -SBINOX $((R,S)$ -**5**) and acyclic analogue **4** lies in the $\text{C}_{\text{core}}-\text{C}-\text{O}-\text{C}_{\text{aryl}}$ torsional angles, which have values of $72.2(3)^\circ$, $-73.2(3)^\circ$, $-121.7(2)^\circ$, and $123.3(2)^\circ$ in SBINOX and only $175.1(2)^\circ$ and $-175.1(2)^\circ$ in model **4**. Nearly full extension of the $\text{C}_{\text{core}}-\text{C}-\text{O}-\text{C}_{\text{aryl}}$ arm is feasible in acyclic model **4**, but only much smaller torsional angles can be accommodated within the constrained spirocyclic core of (R,S) -SBINOX $((R,S)$ -**5**). Further evidence that these constraints have structural consequences is provided by the average value of the interaryl torsional angle ($62.6(2)^\circ$), which is significantly larger than in the structure of the NH_2Et_2^+ salt of (\pm) -spiroborate **3** (53°).⁶

In predicting the behavior of hypothetical tectons derived from SBINOX (**5**), it is helpful to examine how the characteristic geometry of the pentaerythrityl core will determine the orienta-

(20) Crystallization of meso compound (R,S) -**5** in the chiral space group $P2_12_12_1$ is related to the more general phenomenon of achiral molecules that crystallize in non-centrosymmetric space groups. For a recent survey of examples, see: Pidcock, E. *Chem. Commun.* **2005**, 3457–3459.

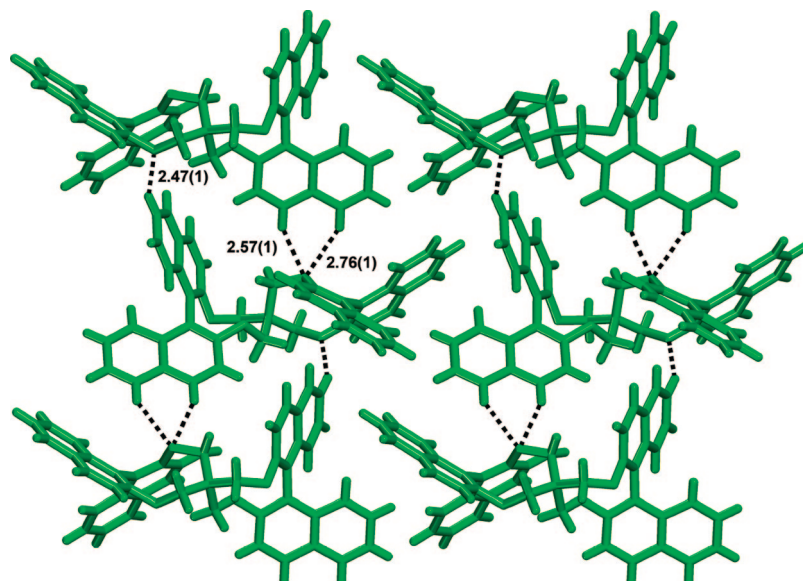


FIGURE 3. Partial view of the structure of crystals of (R,S) -SBINOX ((R,S) -5) grown from CH_2Cl_2 /hexane. For simplification, molecules of (R,S) -SBINOX are drawn with all atoms in green. Broken lines are used to represent key intermolecular $\text{C}-\text{H}\cdots\text{O}$ interactions.

TABLE 1. Crystallographic Data for (R,S) -SBINOX (5), (\pm) -Tetrabromide 6, (S,S) -Tetrabromide 6, and (S,S) -Octabromide 7

compd	(R,S) -5	$2(\pm)$ -6 $\cdot\text{C}_6\text{H}_{14}$	(S,S) -6 $\cdot 2\text{C}_6\text{H}_6$	(S,S) -7 $\cdot 2\text{CH}_2\text{Cl}_2\cdot\text{C}_6\text{H}_{14}$
formula	$\text{C}_{45}\text{H}_{32}\text{O}_4$	$\text{C}_{93}\text{H}_{63}\text{Br}_8\text{O}_8$	$\text{C}_{57}\text{H}_{40}\text{Br}_4\text{O}_4$	$\text{C}_{53}\text{H}_{42}\text{Br}_8\text{Cl}_4\text{O}_4$
formula wt	636.71	1947.71	1108.53	1523.95
crystal system	orthorhombic	triclinic	orthorhombic	orthorhombic
space group	$P2_12_12_1$	$P\bar{1}$	$P2_12_12_1$	$P2_12_12_1$
a (Å)	13.8546(11)	11.4661(2)	12.5871(9)	11.2577(4)
b (Å)	15.2258(14)	15.3621(3)	15.7329(11)	16.6181(6)
c (Å)	15.5191(12)	22.3588(5)	23.1693(16)	28.4719(11)
α (deg)	90	105.206(1)	90	90
β (deg)	90	94.292(1)	90	90
γ (deg)	90	91.621(1)	90	90
V (Å ³)	3273.7(5)	3785.11(13)	4588.3(6)	5326.6(3)
Z	4	2	4	4
T (K)	100(2)	100(2)	100(2)	100(2)
ρ_{calc} (g cm ⁻³)	1.292	1.709	1.605	1.900
λ (Cu K α , Å)	1.54178	1.54178	1.54178	1.54178
μ (Cu K α , mm ⁻¹)	0.645	5.560	4.670	9.415
$R_1, I > 2\sigma(I)$ (all)	0.0497 (0.0530)	0.0541 (0.0979)	0.0314 (0.0320)	0.0517 (0.0518)
$wR_2, I > 2\sigma(I)$ (all)	0.1144 (0.1151)	0.1212 (0.1335)	0.0803 (0.0807)	0.1452 (0.1454)
GoF on F^2	1.039	1.042	1.057	1.064
Flack parameter	-0.1(2)		-0.019(11)	0.02(3)
measured reflections	26747	48322	56065	57351
independent reflections	6403	13247	8339	9813

tion of peripheral sites of intermolecular association. Of primary interest are sites of association introduced by simple methods, such as direct electrophilic substitution of BINOL or its derivatives. The ready availability of 6,6'-dibromo[1,1'-binaphthalene]-2,2'-diol¹⁷ by bromination of BINOL draws special attention to sites of association at the 6,6'-positions. In the observed structure of meso (R,S) -SBINOX ((R,S) -5), the $\text{C}_{\text{N}}\cdots\text{C}_{\text{core}}\cdots\text{C}_{\text{N}}$ angles defined by the central carbon atom of the pentaerythrityl core and the 6, 6', 6'', and 6''' positions of the naphthyl groups (C_{N}) range from 53.5(3)° to 154.1(3)°. Sites of intermolecular association at these positions are therefore expected to deviate markedly from a tetrahedral orientation. In contrast, the two independent $\text{C}_{\text{Ph}}\cdots\text{C}_{\text{core}}\cdots\text{C}_{\text{Ph}}$ angles of acyclic model 4, which are defined by the central carbon atom and the 4, 4', 4'', and 4''' positions of the phenyl groups (C_{Ph}), have the values 87.77(5)° and 121.30(3)°. In the structure of the NH_2Et_2^+ salt of (\pm) -spiroborate 3, the $\text{C}_{\text{N}}\cdots\text{B}_{\text{core}}\cdots\text{C}_{\text{N}}$ angles defined by the central boron atom (B_{core}) and the 6, 6', 6'', and

6''' positions of the naphthyl groups lie in the range 60.0(2)°–152.1(2)°. As a result, tectons derived from the constrained spirocyclic scaffolds of (\pm) -spiroborate 3 and meso (R,S) -SBINOX ((R,S) -5) should have geometries that are well-defined but distinctly different, and association is unlikely to give networks with the same connectivities and architectures.

The structure of crystals of meso (R,S) -SBINOX ((R,S) -5) grown from CH_2Cl_2 /hexane reveals that both 9-membered rings in the spirocycle adopt similar conformations of C_1 symmetry (Figure 2). The conformations closely resemble those observed in other dibenzannulated derivatives of [1,5]dioxonane that have been characterized crystallographically, including spirocycles 8,²¹ 9,²² 10,²³ and 11.²⁴

(21) Stadnicka, K.; Szlachcic, P. *Acta Crystallogr.* **2003**, *C59*, o129–o131.

(22) Stadnicka, K.; Lebioda, Ł. *Acta Crystallogr.* **1979**, *B35*, 2760–2763.

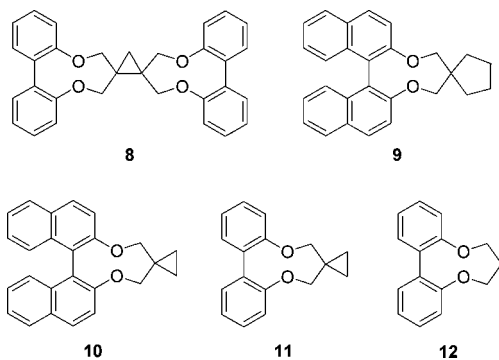
(23) Stadnicka, K. *Acta Crystallogr.* **1979**, *B35*, 2757–2760.

(24) Karle, I. L.; Grochowski, J. *Acta Crystallogr.* **1979**, *B35*, 1293–1295.

TABLE 2. Selected Interatomic Distances and Angles Observed in the Structures of (*R,S*)-SBINOX (**5**), (\pm)-Tetrabromide **6**, (*S,S*)-Tetrabromide **6**, and (*S,S*)-Octabromide **7**

compd	C–C _{core} –C angles (deg)	C _N ···C _{core} ···C _N angles ^b (deg)	C _{core} –C–O–C _{aryl} torsional angles (deg)	short intraannular C–H···O distances (Å)	short interannular C–H···O distances (Å)	interaryl torsional angles ^c (deg)
<i>(R,S)</i> - 5	104.9(2)	53.5(3)	72.2(3)	2.83(1)	2.28(1)	62.0(2)
	108.8(2)	57.5(3)	–73.2(3)	2.79(1)	2.32(1)	63.1(2)
	109.3(2)	98.2(3)	–121.7(2)			
	110.2(2)	99.2(3)	123.2(2)			
	111.5(2)	114.2(3)				
	111.9(2)	154.1(3)				
2 (\pm)- 6 ·C ₆ H ₁₄ ^a	103.2(4)	53.9(5)	75.4(7)	2.70(1)	2.51(1)	58.8(8)
	109.1(4)	56.3(5)	80.7(6)	2.75(1)	2.68(1)	63.7(8)
	110.0(5)	101.3(5)	124.2(5)			
	110.1(5)	109.1(5)	126.1(5)			
	112.0(5)	111.8(5)				
	112.4(5)	147.7(5)				
<i>(S,S)</i> - 6 ·2C ₆ H ₆	106.5(2)	52.5(2)	82.6(3)	2.65(1)	2.41(1)	58.4(4)
	106.7(2)	55.6(2)	83.9(3)	2.73(1)	2.65(1)	60.9(4)
	108.1(2)	86.3(2)	125.6(2)		2.69(1)	
	109.9(2)	116.7(2)	129.1(2)		2.76(1)	
	111.2(2)	125.1(2)				
	114.1(2)	166.7(2)				
<i>(S,S)</i> - 7 ·2CH ₂ Cl ₂ ·C ₆ H ₁₄	103.8(5)	52.4(5)	72.4(7)	2.68(1)	2.57(1)	58.8(9)
	109.9(5)	57.3(5)	88.7(7)	2.81(1)	2.58(1)	61.8(8)
	110.2(5)	96.0(5)	121.5(6)			
	110.2(5)	109.8(5)	130.6(7)			
	111.0(5)	113.6(5)				
	111.8(5)	146.4(5)				

^a Geometric parameters provided for (*S,S*) enantiomer only. ^b Measure of deviation from tetrahedral geometry defined by angles between the central carbon atom of the pentaerythritol core (C_{core}) and the 6, 6', 6'', and 6''' positions of the naphthyl groups (C_N). ^c Measured between the average aryl planes.



Based on analysis of variable-temperature NMR spectra, Rhys and Duddeck proposed a *C*₂ conformation for compound **12**.²⁵ However, because every other member of this family unambiguously favors a conformation of lower symmetry in the solid state, we suggest that compound **12** also prefers a *C*₁ conformation but that a less stable alternative conformation of *C*₂ symmetry is energetically accessible. This would account for the apparent symmetry revealed by NMR experiments in the case of compound **12**, as well as in the cases of SBINOX (**5**) and its brominated derivatives **6** and **7** (Figure 1).

A noteworthy feature, clearly visible in the structures of the 9-membered rings of meso (*R,S*)-SBINOX ((*R,S*)-**5**) and analogues **8–11** but not noted in previous crystallographic studies,^{21–24} is the presence of characteristic intraannular C–H···O interactions.²⁶ These interactions, which define a

5-membered ring linking an oxygen atom of each dioxonane ring with a transannular CH₂ group,²⁷ presumably play a role in stabilizing the preferred *C*₁ conformations. In meso (*R,S*)-SBINOX ((*R,S*)-**5**), one such interaction is observed within each dioxonane ring, with H···O distances of 2.79(1) and 2.83(1) Å. Similar H···O distances (2.76–3.00 Å) are observed in the dioxonane rings of models **8–11**.^{21–24} However, (*R,S*)-SBINOX differs from these simple analogues because the unique topology of spiroannulated dioxonane rings allows the formation of two important new intramolecular C–H···O interactions, both involving one oxygen atom of each dioxonane and a hydrogen atom of a CH₂ group in the other 9-membered ring (Figure 2).²⁷ The resulting H···O distances are very short (2.28(1) and 2.32(1) Å), suggesting that these interactions help determine the overall shape of the (*R,S*)-SBINOX scaffold. The same hydrogen atoms involved in these distinctive C–H···O interactions also engage in intramolecular interannular C–H··· π interactions with nearby naphthyl rings (shortest H···C distances of 2.76(1) and 2.83(1) Å). An additional aromatic C–H···O interaction (2.82(1) Å) further stabilizes the observed conformation.²⁷ Together, these multiple interactions create a well-ordered structure and may help account for the relatively large separation ($\Delta\delta = 0.34$) of the CH₂ doublets in the ¹H NMR spectrum of meso (*R,S*)-SBINOX ((*R,S*)-**5**).

Despite the irregular cruciform shape created by two spiroannulated 9-membered rings, the crystal structure of meso (*R,S*)-SBINOX ((*R,S*)-**5**) proved to be close-packed, with no space available for the inclusion of guests. In the structure, intermolecular edge-to-face aromatic interactions are prominent, as well as various C–H···O interactions with H···O distances ranging from 2.47(1) to 2.76(1) Å (Figure 3).

(27) See the Supporting Information for additional details.

(25) Rys, B.; Duddeck, H. *Magn. Reson. Chem.* **1995**, *33*, 110–112.

(26) The ability of C–H bonds to participate in weak hydrogen bonds has been reviewed by: Desiraju, G. R. *Chem. Commun.* **2005**, 299, 5–3001. Desiraju, G. R. *Acc. Chem. Res.* **2002**, *35*, 565–573. Desiraju, G. R.; Steiner, T. *The Weak Hydrogen Bond in Structural Chemistry and Biology*; Oxford University Press: Oxford, 1999.

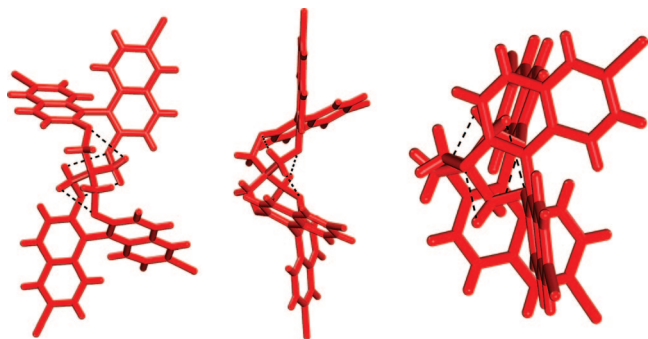


FIGURE 4. Views of the molecular structure of the (*S,S*) isomer of tetrabromide **6** as found in crystals of (\pm)-**6** grown from CH_2Cl_2 /hexane. The structure is viewed along each of three axes of approximate C_2 symmetry. For simplification, all atoms are drawn in red. The four short intramolecular $\text{C}-\text{H}\cdots\text{O}$ interactions are highlighted by broken lines. Guest molecules of hexane are omitted for clarity.

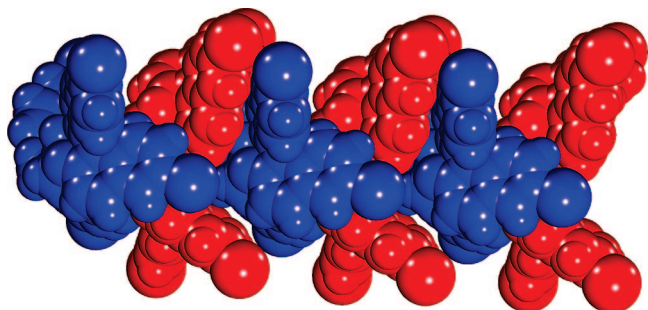


FIGURE 5. Representation of the structure of crystals of (\pm)-tetrabromide **6** grown from CH_2Cl_2 /hexane, showing a column of alternating (*S,S*) and (*R,R*) isomers lying parallel to the *a*-axis. To simplify interpretation, (*S,S*) isomers are drawn with all atoms in red and (*R,R*) isomers with all atoms in blue. All atoms are shown as spheres of van der Waals radii, and guests are omitted for clarity.

Structure of Racemic Tetrabromide 6 ((\pm)-6**).** Crude tetrabromide **6**, obtained as a statistical mixture of the (*S,S*), (*R,S*), and (*R,R*) isomers from the reaction of (\pm)-6,6'-dibromo[1,1'-binaphthalene]-2,2'-diol¹⁷ with pentaerythrityl tetraosylate, was crystallized by exposing a solution in CH_2Cl_2 to vapors of hexane. In this case, the resulting crystals were found to consist of a racemic mixture of the (*S,S*) and (*R,R*) isomers, and the meso (*R,S*) isomer was not present. This observation is consistent with the general tendency of racemic mixtures to crystallize as racemic crystals containing equal amounts of both enantiomers, rather than as conglomerates of crystals that are each composed of a single enantiomer.²⁸ The crystals proved to have the composition 2 **6**·1 hexane and to belong to the triclinic space group $P\bar{1}$. Views of the structure are provided in Figures 4–6, and crystallographic details appear in Tables 1 and 2.

The structures of the (*S,S*) and (*R,R*) isomers of tetrabromide **6** that define the asymmetric unit are not mirror images, but they are closely related,^{27,29} and only the (*S,S*) isomer will be described in detail (Figure 4). Its central $\text{C}(\text{CH}_2\text{O})_4$ unit has a slightly distorted tetrahedral geometry similar to that of the meso (*R,S*) isomer of SBINOX (**5**), and the $\text{C}-\text{C}_{\text{core}}-\text{C}$ angles range from $103.2(4)^\circ$ to $112.4(5)^\circ$. The $\text{C}_{\text{core}}-\text{C}-\text{O}-\text{C}_{\text{aryl}}$ torsional

angles in the (*S,S*) isomer of tetrabromide **6** have values of $75.4(7)^\circ$, $80.7(6)^\circ$, $124.2(5)^\circ$, and $126.1(5)^\circ$, so they resemble those of (*R,S*)-SBINOX ((*R,S*)-**5**). The average value of the interaryl torsional angle in (*S,S*)-tetrabromide **6** is $61.3(8)^\circ$, which is similar to that found in (*R,S*)-SBINOX ($62.6(2)^\circ$) but much larger than that observed in related derivatives of BINOL such as the NH_2Et_2^+ salt of (\pm)-spiroborate **3** (53°).⁶ Together, these data suggest that the [9,9]-spirocyclic cores of SBINOX (**5**) and its derivatives impose particular conformational constraints, but the (*R,S*) and (*S,S*) isomers can accommodate these constraints almost equally well and do not differ greatly in stability. This is consistent with our observation that nearly statistical mixtures of (*S,S*), (*R,S*), and (*R,R*) isomers arise when (\pm)-BINOL and its derivatives react with pentaerythrityl tetraosylate. In contrast, the potentially reversible reaction of boric acid with (\pm)-BINOL leads only to the (*S,S*) and (*R,R*) isomers of spiroborate **3**.⁶ In the [7,7]-spirocyclic series, the (*R,S*) isomer may therefore be significantly less stable, possibly in part because of stereoelectronic effects within the $\text{B}(\text{OC})_4$ core.³⁰

The chiral form of SBINOX (**5**) provides a scaffold that can have D_2 symmetry with three axes of C_2 symmetry. Figure 4 shows (*S,S*)-tetrabromide **6** as viewed along each of these axes. The (*S,S*) isomers of spiroborate **3** and SBINOX (**5**) are constructed from related components and have the same symmetry. However, the overall topologies of the two scaffolds differ, partly, because scaffold **3** incorporates a [7,7]-spirocyclic core, whereas scaffold **5** has a [9,9]-spirocyclic core. In (*S,S*)-tetrabromide **6**, the $\text{C}_N\cdots\text{C}_{\text{core}}\cdots\text{C}_N$ angles (defined by the central carbon atom and the peripheral 6, 6', 6'', and 6''' positions of the naphthyl groups) lie in the range $53.9(5)^\circ$ – $147.7(5)^\circ$, whereas those in (*R,S*)-SBINOX ((*R,S*)-**5**) and the NH_2Et_2^+ salt of (*S,S*)-spiroborate **3** have values in the range $53.5(3)^\circ$ – $154.1(3)^\circ$ and $60.0(2)^\circ$ – $152.1(2)^\circ$, respectively. These parameters are not dramatically different, but they may prevent tectons derived from the three scaffolds from associating to form similar networks.

The structure of crystals of (\pm)-tetrabromide **6** grown from CH_2Cl_2 /hexane confirms that the 9-membered rings adopt conformations similar to those observed in the structure of (*R,S*)-SBINOX ((*R,S*)-**5**) and in models **8**–**12**. The overall shape of (*S,S*)-tetrabromide **6** is maintained in part by four key intramolecular $\text{C}-\text{H}\cdots\text{O}$ hydrogen bonds, with $\text{H}\cdots\text{O}$ distances of 2.51(1) Å, 2.68(1) Å, 2.70(1) Å, and 2.75(1) Å (Figure 4).²⁷ Additional stabilization is provided by intramolecular $\text{C}-\text{H}\cdots\pi$ interactions involving CH_2 groups and nearby naphthyl rings ($\text{H}\cdots\text{C}$ distances of 2.58(1) Å and 2.76(1) Å, with corresponding distances to the centroids of 2.88(1) Å and 3.19(1) Å). An unexpected structural feature in both (*S,S*)- and (*R,R*)-tetrabromide **6** is the presence of a short interannular $\text{O}\cdots\text{O}$ contact (2.903(5) Å in (*S,S*)-**6**), which is only slightly longer than the intraannular $\text{O}\cdots\text{O}$ distances (2.785(5) Å and 2.855(5) Å). In contrast, all other interannular $\text{O}\cdots\text{O}$ distances in (*S,S*)-tetrabromide **6** or in (*R,S*)-SBINOX ((*R,S*)-**5**) exceed 3.62 Å.

The crystal structure of (\pm)-tetrabromide **6** can be described as consisting of columns of alternating (*S,S*) and (*R,R*) isomers, which lie parallel to the *a*-axis (Figure 5).²⁷ Cohesion within the heterochiral columns is maintained in part by multiple $\text{C}-\text{H}\cdots\text{O}$ interactions ($\text{H}\cdots\text{O}$ distances of 2.49(1), 2.51(1), 2.55(1), 2.69(1), 2.74(1) Å, and 2.80(1) Å) and edge-to-face

(28) Jacques, J.; Collet, A.; Wilen, S. H. *Enantiomers, Racemates, and Resolutions*; Wiley: New York, 1981.

(29) The (*S,S*) and (*R,R*) isomers of tetrabromide **6** that define the asymmetric unit (along with 0.5 C_6H_{14}) are not related by the inversion center, so they give rise to two additional inverted molecules in the unit cell.

(30) Xu, Z.; Zhao, C.; Lin, Z. *J. Chem. Soc., Perkin Trans. 2* **2000**, 2319–2323. Gillespie, R. J.; Bytheway, I.; Robinson, E. A. *Inorg. Chem.* **1998**, *37*, 2811–2825. Narasimhamurthy, N.; Manohar, H.; Samuelson, A. G.; Chandrasekhar, J. *J. Am. Chem. Soc.* **1990**, *112*, 2937–2941.

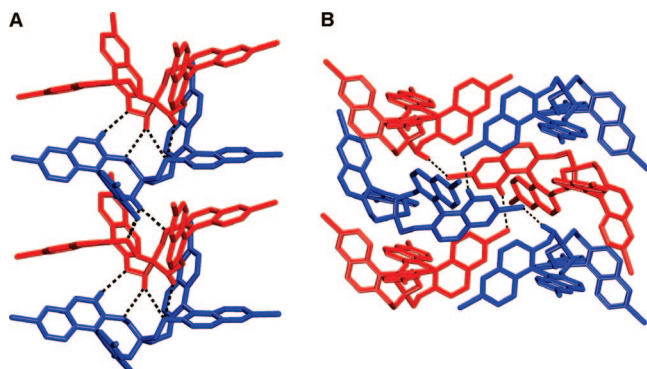


FIGURE 6. (A) View of the structure of crystals of (\pm)-tetrabromide **6** grown from CH_2Cl_2 /hexane, with intermolecular $\text{C}-\text{H}\cdots\text{O}$ interactions shown as broken lines between adjacent (S,S) and (R,R) isomers within a single column. (B) Similar view with intermolecular $\text{C}-\text{H}\cdots\text{Br}$ interactions shown as broken lines between adjacent columns. In both views, (S,S) isomers are drawn with all atoms in red and (R,R) isomers with all atoms in blue. Guests and hydrogen atoms not involved in intermolecular hydrogen bonding are omitted for clarity.

aromatic interactions. Contacts between adjacent columns involve $\text{C}-\text{H}\cdots\text{Br}$ interactions (2.79(1) Å and 2.84(1) Å), $\text{Br}\cdots\text{Br}$ interactions (3.398(5) Å), $\text{Br}\cdots\pi$ interactions, and edge-to-face aromatic interactions (Figure 6). The structure includes hexane, and approximately 8% of the volume is accessible to guests, as measured by standard methods.^{31,32} The observation that meso (R,S)-SBINOX ((R,S)-**5**) crystallizes as a close-packed structure, whereas (\pm)-tetrabromide **6** crystallizes under similar conditions with included guests, is consistent with differences between tetraaryl-substituted hydrocarbons and their halogenated derivatives noted earlier by Bishop and co-workers.³³

Structure of (S,S)-Tetrabromide 6. (S,S)-Tetrabromide **6**, obtained enantiomerically pure from the reaction of (S)-6,6'-dibromo[1,1'-binaphthalene]-2,2'-diol¹⁷ with pentaerythrityl tetraosylate, was crystallized by exposing a solution in CH_2Cl_2 to vapors of benzene. The crystals were found to have the composition **6**·2 benzene and to belong to the orthorhombic space group $P2_12_12_1$. Views of the structure appear in Figures 7–8, and crystallographic details are provided in Tables 1 and 2.

In crystals of both the pure enantiomer and the racemate, both dioxonane rings of (S,S)-tetrabromide **6** adopt the standard conformation. Nevertheless, the overall topology of (S,S)-**6** is distinctly different in crystals of the pure enantiomer and in crystals of the racemate, because the two rings are arrayed differently around the spirocyclic carbon atom (C_{core}). This difference is illustrated by the superimposed structures shown in Figure 7. The variation underscores the inherent flexibility of the dioxonane core and the challenge of using SBINOX scaffolds to orient substituents predictably, despite the presence of multiple intramolecular $\text{C}-\text{H}\cdots\text{O}$ hydrogen bonds and other interactions that help favor consistent conformational preferences.

(31) The percentage of volume accessible to guests was estimated by the PLATON program.³² PLATON calculates the accessible volume by allowing a spherical probe of variable radius to roll over the van der Waals surface of the network. PLATON uses a default value of 1.20 Å for the radius of the probe, which is an appropriate model for small guests such as water. The van der Waals radii used to define surfaces for these calculations are as follows: C, 1.70 Å; H, 1.20 Å; Br, 1.85 Å; O, 1.52 Å. The percentage of accessible volume is given by $100 V_{\text{g}}/V$, where V is the volume of the unit cell and V_{g} is the guest-accessible volume as calculated by PLATON.

(32) Spek, A. L. *PLATON, A Multipurpose Crystallographic Tool*; Utrecht University: Utrecht, The Netherlands, 2007. van der Sluis, P.; Spek, A. L. *Acta Crystallogr.* **1990**, *A46*, 194–201.

(33) Marjo, C. E.; Rahman, A. N. M. M.; Bishop, R.; Scudder, M. L.; Craig, D. C. *Tetrahedron* **2001**, *57*, 6289–6293.

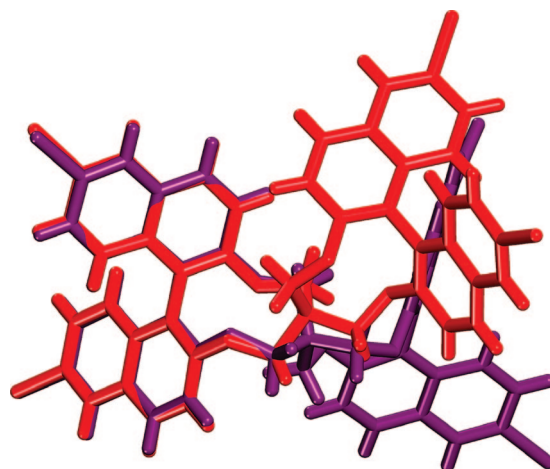


FIGURE 7. Superposition of the molecular structures of (S,S)-tetrabromide **6**, as observed in crystals of the enantiomerically pure compound and the racemate. The structures are shown with all atoms drawn in purple (enantiomerically pure crystals) and in red (racemic crystals).

The structure of (S,S)-tetrabromide **6** reveals six key intramolecular $\text{C}-\text{H}\cdots\text{O}$ interactions, with $\text{H}\cdots\text{O}$ distances in the range 2.41(1)–2.76(1) Å.²⁷ In addition, there are two important intramolecular $\text{C}-\text{H}\cdots\pi$ interactions involving CH_2 groups and nearby naphthyl rings, with $\text{H}\cdots\text{C}$ distances of 2.70(1) and 2.90(1) Å and corresponding distances to the centroids of 3.14(1) and 3.38(1) Å. Unlike the (S,S) isomer in racemic crystals of (\pm)-tetrabromide **6**, which incorporates a short interannular $\text{O}\cdots\text{O}$ contact (2.903(5) Å), the (S,S) isomer in enantiomerically pure crystals has no interannular $\text{O}\cdots\text{O}$ distances shorter than 4.08 Å. Again, the central $\text{C}(\text{CH}_2\text{O})_4$ unit has a slightly distorted tetrahedral geometry, with $\text{C}-\text{C}_{\text{core}}-\text{C}$ angles varying from 106.5(2)° to 114.1(2)°. The $\text{C}_{\text{core}}-\text{C}-\text{O}-\text{C}_{\text{aryl}}$ torsional angles have values of 82.6(3)°, 83.9(3)°, 125.6(2)°, and 129.1(2)°, so they closely resemble those observed in the structure of (\pm)-tetrabromide **6**. The average value of the interaryl torsional angle is 59.3(4)°, which is similar to that found in the racemic crystal (61.3(7)°). The $\text{C}_{\text{N}}\cdots\text{C}_{\text{core}}\cdots\text{C}_{\text{N}}$ angles, which help define the orientation of substituents at the 6, 6', 6'', and 6''' positions of the naphthyl groups, have values in the range 52.5(2)–166.7(2)°.

Cohesion of crystals of (S,S)-tetrabromide **6** grown from CH_2Cl_2 /benzene is maintained in part by intermolecular $\text{C}-\text{H}\cdots\text{Br}$ interactions (2.91(1) and 2.96(1) Å), $\text{C}-\text{H}\cdots\text{O}$ interactions ($\text{H}\cdots\text{O}$ distances of 2.14(1), 2.49(1), and 2.54(1) Å), $\text{Br}\cdots\pi$ interactions (3.514(1) and 3.633(1) Å), and $\text{C}-\text{H}\cdots\pi$ interactions (Figure 8). The structure includes benzene, and approximately 27% of the volume is accessible to guests, as measured by standard methods.^{31,32} Crystals of (S,S)-tetrabromide **6** incorporate fewer significant intermolecular interactions than do crystals of (\pm)-tetrabromide **6**, and the volume accessible to guests is higher, suggesting that packing in the enantiomerically pure crystals is less efficient than in the racemic crystals.

Structure of (S,S)-Octabromide 7. (S,S)-Octabromide **7**, synthesized in enantiomerically pure form by the reaction of (S)-4,4',6,6'-tetrabromo[1,1'-binaphthalene]-2,2'-diol^{18,19} with pentaerythrityl tetraosylate, was crystallized by exposing a solution in CH_2Cl_2 to vapors of hexane. The crystals proved to have the composition **7**·2 CH_2Cl_2 ·1 hexane and to belong to the orthorhombic space group $P2_12_12_1$. Views of the structure appear in Figures 9 and 10 and crystallographic details are provided in Tables 1 and 2.

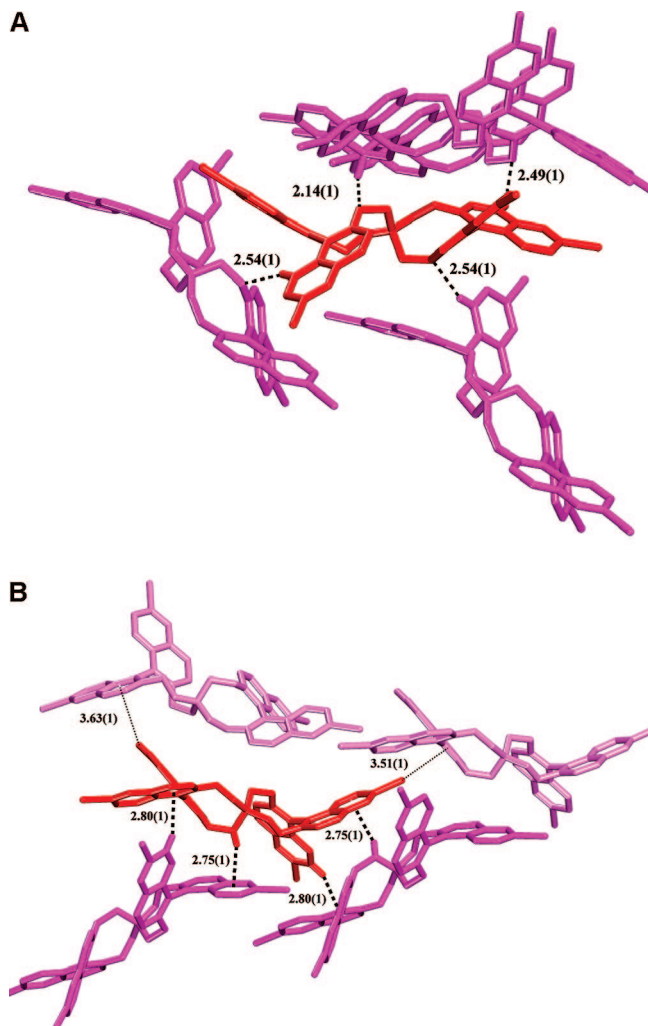


FIGURE 8. Views of selected intermolecular interactions observed in crystals of (*S,S*)-tetrabromide **6** grown from $\text{CH}_2\text{Cl}_2/\text{benzene}$. (A) $\text{C-H}\cdots\text{O}$ interactions involving a central molecule (red) and four neighbors (pink). (B) View of a central molecule (red), showing $\text{Br}\cdots\pi$ interactions with two neighbors (light pink) and $\text{C-H}\cdots\pi$ interactions with two other neighbors (darker pink). In both views, broken lines are used to represent intermolecular interactions. Guests and hydrogen atoms are omitted for clarity, except those involved in intermolecular hydrogen bonding.

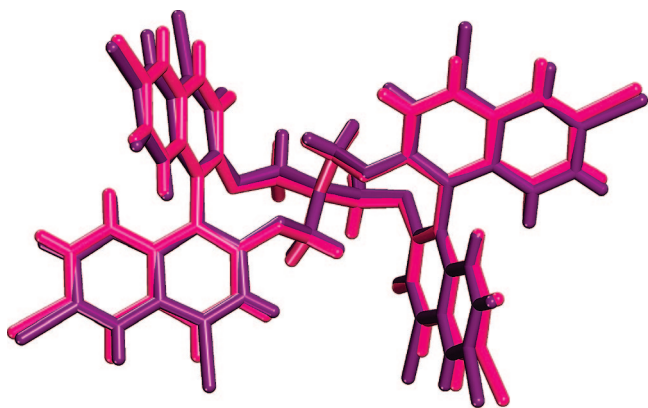


FIGURE 9. Superposition of the molecular structures of (*S,S*)-tetrabromide **6** and (*S,S*)-octabromide **7**. The structures are shown with all atoms drawn in pink ((*S,S*)-tetrabromide **6**) and in contrasting purple ((*S,S*)-octabromide **7**).

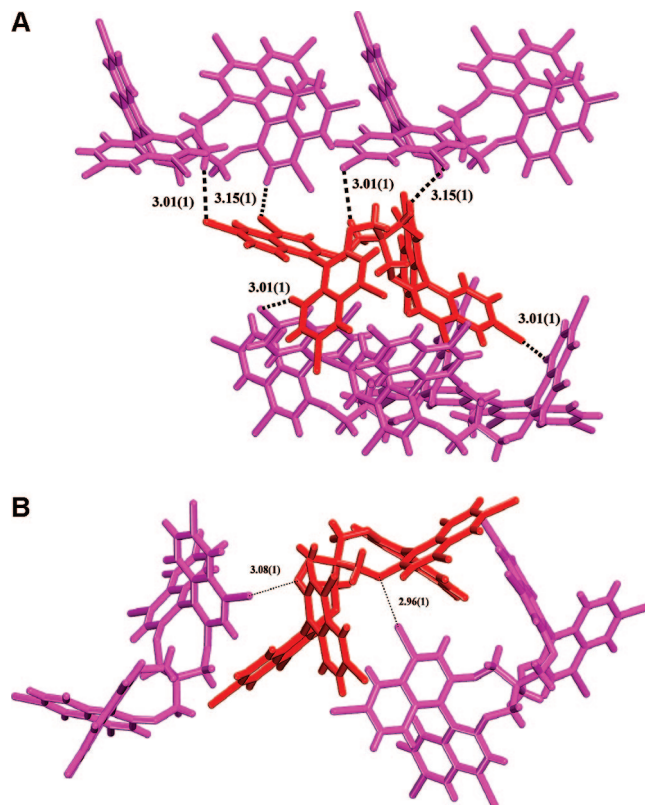


FIGURE 10. View of selected intermolecular interactions found in crystals of (*S,S*)-octabromide **7** grown from $\text{CH}_2\text{Cl}_2/\text{hexane}$. (A) $\text{C-H}\cdots\text{Br}$ interactions involving a central molecule (red) with four neighbors (pink). (B) $\text{Br}\cdots\text{O}$ interactions of a central molecule (red) with two neighbors (pink). In both views, broken lines are used to represent intermolecular interactions. Guests and hydrogen atoms are omitted for clarity, except those involved in intermolecular hydrogen bonding.

(*S,S*)-Octabromide **7** maintains the geometry of the (*S,S*)-SBINOX scaffold observed in (*S,S*)-tetrabromide **6**, and a superposition of molecular structures is shown in Figure 9. It is noteworthy that the basic conformation of the core is conserved despite octasubstitution of the peripheral naphthyl groups. Four significant intramolecular $\text{C-H}\cdots\text{O}$ interactions are present in the structure of octabromide **7**, with $\text{H}\cdots\text{O}$ distances ranging from 2.57(1) to 2.81(1) Å.²⁷ Like the (*S,S*) isomer in crystals of (\pm)-tetrabromide **6**, the (*S,S*) isomer in crystals of enantiomerically pure octabromide **7** contains an unusually short interannular $\text{O}\cdots\text{O}$ contact (2.91(1) Å). In addition, there are two key intramolecular $\text{C-H}\cdots\pi$ interactions involving CH_2 groups and nearby naphthyl rings, with $\text{H}\cdots\text{C}$ distances of 2.52(1) and 2.86(1) Å and corresponding distances to the centroids of 2.81(1) and 3.36(1) Å. As usual, the central $\text{C}(\text{CH}_2\text{O})_4$ unit has a slightly distorted tetrahedral geometry, with $\text{C-C}_{\text{core}}-\text{C}$ angles varying from 103.8(5)° to 111.8(5)°. The $\text{C}_{\text{core}}-\text{C}-\text{O}-\text{C}_{\text{aryl}}$ torsional angles are 72.4(7), 88.7(7), 121.5(6), and 130.6(7)°, so they are similar to those found in other derivatives of (*S,S*)-SBINOX. The average value of the interaryl torsional angle (60.3(8)°) is also typical of derivatives of SBINOX, and the $\text{C}_{\text{N}}\cdots\text{C}_{\text{core}}\cdots\text{C}_{\text{N}}$ angles between the core and the 6, 6', 6'', and 6''' positions of the naphthyl substituents are normally divergent (52.4(5)–146.4(5)°).

Diverse intermolecular interactions are present in crystals of (*S,S*)-octabromide **7** grown from $\text{CH}_2\text{Cl}_2/\text{hexane}$ (Figure 10). Those judged to be particularly significant include $\text{C-H}\cdots\text{Br}$ interactions (3.01(1) and 3.15(1) Å), $\text{Br}\cdots\text{O}$ contacts (2.96(1) and 3.08(1) Å), $\text{Br}\cdots\pi$ interactions, and $\text{C-H}\cdots\pi$ interactions.

In addition, there are C–H···O interactions and C–H···Cl interactions involving included molecules of CH₂Cl₂. Despite the high degree of bromination of compound **7** and the importance of halogen–halogen interactions in other molecular crystals,^{33,34} no intermolecular Br···Br distances shorter than 3.90 Å are present. The structure includes both CH₂Cl₂ and hexane, and approximately 31% of the volume is accessible to guests, as measured by standard methods.^{31,32}

Conclusions

Our work has established that SBINOX (**5**) and its derivatives can be prepared conveniently in high yield and in stereoisomerically pure (*S,S*), (*R,S*), and (*R,R*) forms. The 9-membered dioxonane rings in these structures adopt characteristic conformations of C₁ symmetry, as observed previously in simple models. Intraannular C–H···O interactions help maintain the conformations of the individual rings, and the overall geometry of the spirocyclic SBINOX core is controlled in part by distinctive short interannular C–H···O and C–H···π interactions. Derivatives of SBINOX (**5**) can therefore be expected to orient peripheral substituents in characteristic ways, despite the inherent flexibility of the dioxonane core. For these reasons, SBINOX (**5**) is a potentially useful scaffold for applications in drug discovery, crystal engineering, and related fields.

Experimental Section

General Procedure for the Synthesis of SBINOX (5**) and Its Derivatives.** A mixture of pentaerythryl tetratosylate (940 mg, 1.25 mmol),³⁵ a suitable derivative of [1,1'-binaphthalene]-2,2'-diol (2.50 mmol), and K₂CO₃ (5.10 mmol) in DMF (20 mL) was stirred and heated at 120 °C for 24 h. The hot mixture was allowed to cool, and H₂O (20 mL) was added. The precipitated solid was separated by filtration and dissolved in CH₂Cl₂. The solution was washed with H₂O and brine and was then dried over anhydrous Na₂SO₄. Removal of volatiles under reduced pressure left a residue that was then purified by flash chromatography.

Synthesis of SBINOX (5**).** Use of (±)-[1,1'-binaphthalene]-2,2'-diol in the general procedure gave a crude product that was purified by chromatography (silica, CH₂Cl₂/hexane 7:3, *R_f* = 0.50) to give SBINOX (**5**) in 85% yield as a colorless solid composed of a nearly statistical 1:2:1 mixture of the (*S,S*), (*R,S*), and (*R,R*) stereoisomers: IR (KBr) 3057, 2951, 2882, 1676, 1591, 1506, 1325, 1224, 1076, 1008, 812, 746 cm⁻¹; ¹H NMR (400 MHz, CDCl₃, 298 K) δ 8.02 (d, ³*J* = 8.8 Hz, 4H), 7.94–7.89 (m, 12H), 7.42–7.18 (m, 32H), 4.41 (d, ²*J* = 11.8 Hz, 4H), 4.22 (d, ²*J* = 12.0 Hz, 4H), 4.15 (d, ²*J* = 12.0 Hz, 4H), 4.06 (d, ²*J* = 11.9 Hz, 4H); HRMS (APCI) calcd for C₄₅H₃₂O₄ + H *m/e* 637.2373, found 637.2382.

Synthesis of (*S,S*)-SBINOX ((*S,S*)-5**).** Use of (*S*)-[1,1'-binaphthalene]-2,2'-diol in the general procedure gave a crude product that was purified by chromatography (silica, CH₂Cl₂/hexane 7:3, *R_f* = 0.50) to give (*S,S*)-SBINOX ((*S,S*)-**5**) as a colorless solid in 75% yield: mp >300 °C; [α]_D²⁰ +137.0 (*c* = 0.620, CH₂Cl₂); IR (KBr) 3057, 2951, 2883, 1676, 1591, 1506, 1325, 1224, 1076, 1008, 812, 746 cm⁻¹; ¹H NMR (400 MHz, CDCl₃, 298 K) δ 8.02 (d, ³*J* = 8.8 Hz, 4H), 7.94–7.89 (m, 4H), 7.42–7.19 (m, 16H), 4.22 (d, ²*J* = 12.0 Hz, 4H), 4.15 (d, ²*J* = 12.0 Hz, 4H); ¹³C NMR (100 MHz, CDCl₃, 298 K) δ 155.5, 133.4, 130.4, 129.7, 128.1, 126.5, 126.3, 124.3, 122.1, 119.0, 73.8, 52.6; HRMS (APCI) calcd for C₄₅H₃₂O₄ + H *m/e* 637.2373, found 637.2367. Anal. Calcd for 3C₄₅H₃₂O₄ · 1CH₂Cl₂: C, 81.87; H, 4.95. Found: C, 81.50; H, 5.23.

Synthesis of Tetrabromide **6.** Use of (±)-6,6'-dibromo[1,1'-binaphthalene]-2,2'-diol¹⁷ in the general procedure gave a crude product that was purified by chromatography (silica, CH₂Cl₂/hexane 4:6, *R_f* = 0.45) to give tetrabromide **6** in 60% yield as a colorless solid composed of a nearly statistical 1:2:1 mixture of the (*S,S*), (*R,S*), and (*R,R*) stereoisomers: IR (KBr) 2947, 2372, 1585, 1506, 1492, 1323, 1238, 1020, 871, 810 cm⁻¹; ¹H NMR (300 MHz, CDCl₃, 298 K) δ 8.09 (d, ⁴*J* = 1.9 Hz, 4H), 8.06 (d, ⁴*J* = 1.9 Hz, 4H), 7.92 (d, ³*J* = 9.0 Hz, 4H), 7.84 (d, ³*J* = 9.0 Hz, 4H), 7.39–7.28 (m, 16H), 7.11 (d, ³*J* = 9.0 Hz, 4H), 7.01 (d, ³*J* = 9.0 Hz, 4H), 4.38 (d, ²*J* = 12.2 Hz, 4H), 4.17 (d, ²*J* = 11.9 Hz, 4H), 4.12 (d, ²*J* = 11.9 Hz, 4H), 4.04 (d, ²*J* = 12.2 Hz, 4H); HRMS (APCI) calcd for C₄₅H₂₈Br₄O₄ + H *m/e* 948.8794, found 948.8772. Anal. Calcd for C₄₅H₂₈Br₄O₄: C, 56.75; H, 2.96. Found: C, 57.18; H, 3.31.

Synthesis of (*S,S*)-Tetrabromide **6.** Use of (*S*)-6,6'-dibromo[1,1'-binaphthalene]-2,2'-diol¹⁷ in the general procedure gave a crude product that was purified by chromatography (silica, CH₂Cl₂/hexane 4:6, *R_f* = 0.45) to give (*S,S*)-tetrabromide **6** in 55% yield as a colorless solid: mp 295 °C; [α]_D²⁰ +191.3 (*c* = 0.275, CH₂Cl₂); IR (KBr) 2953, 1645, 1581, 1492, 1323, 1236, 1020, 877, 810 cm⁻¹; ¹H NMR (400 MHz, CDCl₃, 298 K) δ 8.09 (d, ⁴*J* = 1.8 Hz, 4H), 7.92 (d, ³*J* = 8.9 Hz, 4H), 7.37 (d, ³*J* = 8.9 Hz, 4H), 7.31 (dd, ³*J* = 9.1 Hz, ⁴*J* = 1.8 Hz, 4H), 7.01 (d, ³*J* = 9.1 Hz, 4H), 4.17 (d, ²*J* = 11.9 Hz, 4H), 4.12 (d, ²*J* = 11.9 Hz, 4H); ¹³C NMR (100 MHz, CDCl₃, 298 K) δ 157.1, 132.9, 132.8, 131.4, 131.1, 130.3, 129.2, 123.0, 121.1, 119.7, 74.3, 52.6; HRMS (APCI) calcd for C₄₅H₂₈Br₄O₄ *m/e* 948.8794, found 948.8780. Anal. Calcd for C₄₅H₂₈Br₄O₄: C, 56.75; H, 2.96. Found: C, 56.73; H, 3.08.

Synthesis of (*S,S*)-Octabromide **7.** Use of (*S*)-4,4',6,6'-tetrabromo[1,1'-binaphthalene]-2,2'-diol^{18,19} in the general procedure gave a crude product that was purified by chromatography (silica, CH₂Cl₂/hexane 4:6, *R_f* = 0.50) to give (*S,S*)-octabromide **7** in 25% yield as a colorless solid: mp >350 °C; [α]_D²⁰ +252.9 (*c* = 0.095, CH₂Cl₂); IR (KBr) 2928, 2872, 1582, 1485, 1307, 1215, 1080, 1008, 929, 813 cm⁻¹; ¹H NMR (400 MHz, benzene-*d*₆, 298 K) δ 8.73 (d, ⁴*J* = 1.9 Hz, 4H), 7.44 (s, 4H), 7.10 (dd, ³*J* = 9.0 Hz, ⁴*J* = 1.9 Hz, 4H), 6.82 (d, ³*J* = 9.0 Hz, 4H), 3.56 (d, ²*J* = 11.8 Hz, 4H), 3.24 (d, ²*J* = 11.8 Hz, 4H); ¹³C NMR (100 MHz, benzene-*d*₆, 298 K) δ 155.9, 132.7, 131.5, 130.8, 130.3, 124.4, 123.2, 121.7, 121.2, 72.7, 52.5; HRMS (APCI) calcd for C₄₅H₂₄Br₈O₄ + Cl⁻ *m/e* 1294.4835, found 1294.4854. Anal. Calcd for C₄₅H₂₄Br₈O₄ · 1.5 hexane: C, 46.42; H, 3.25. Found: C, 46.32; H, 3.17.

X-ray Crystallographic Studies. Data were collected using (1) a Bruker AXS SMART 4K/Platform diffractometer or (2) a Bruker AXS SMART 2K/Platform diffractometer with Cu Kα radiation at 100 K. Structures were solved by direct methods using SHELXS-97 and refined using SHELXL-97.³⁶ All non-hydrogen atoms were refined anisotropically, whereas hydrogen atoms were placed in calculated positions and defined as riding atoms.

Acknowledgment. We are grateful to the Natural Sciences and Engineering Research Council of Canada, the Ministère de l'Éducation du Québec, the Canada Foundation for Innovation, the Canada Research Chairs Program, and Université de Montréal for financial support. We thank Prof. Jurgen Sygusch for providing access to a diffractometer equipped with a rotating anode.

Supporting Information Available: Additional crystallographic details, including ORTEP drawings and tables of structural data. This material is available free of charge via the Internet at <http://pubs.acs.org>.

JO800215W

(34) For references, see Metrangolo, P.; Neukirch, H.; Pilati, T.; Resnati, G. *Acc. Chem. Res.* **2005**, *38*, 386–395.

(35) Shostakovskii, M. F.; Atavin, A. S.; Mirskova, A. N. *Zh. Obshch. Khim.* **1965**, *35*, 804–807.

(36) Sheldrick, G. M. *SHELXS-97, Program for the Solution of Crystal Structures and SHELXL-97, Program for the Refinement of Crystal Structures*; Universität Göttingen: Germany, 1997.